Effects of intersite Coulomb interaction on ferromagnetism and dimerization in nanographite ribbons

INSTITUTE OF PHYSICS PUBLISHING JOURNAL OF PHYSICS: CONDENSED MATTER

J. Phys.: Condens. Matter **18** (2006) 6273–6280 doi:10.1088/0953-8984/18/27/010

Effects of intersite Coulomb interaction on ferromagnetism and dimerization in nanographite ribbons

L Y Zhu and W Z Wang[1]

Department of Physics, Wuhan University, Wuhan 430072, People's Republic of China

E-mail: wzwang@whu.edu.cn

Received 3 April 2006, in final form 30 May 2006
Published 23 June 2006
Online at stacks.iop.org/JPhysCM/18/6273

Abstract

Using the Peierls-extended Hubbard model and Hartree–Fock approximation, the stability and dimerization of the ferromagnetic ground state of a nanographite ribbon are investigated. For a given on-site Coulomb interaction U, if the intersite Coulomb interaction V is larger than a critical value V_c, the ferromagnetic ground state is unstable and a transition from the spin-density-wave state to the charge-density-wave state occurs. On increasing the width of the ribbon, the critical value V_c changes from $V_c \approx 0.5U$ to $V_c \approx 0.25U$, which are similar values to those in the one- and two-dimensional extended Hubbard model, respectively. The on-site repulsion usually suppresses the dimerization while the intersite repulsion can turn the dimerization on and off.

1. Introduction

For the last couple of decades, the synthesis of organic molecular ferromagnetic compounds [1–5] has attracted considerable attention. Recently, the reports on carbon polymer have stimulated renewed interest in carbon systems as possible new magnetic materials made of light elements [6–8]. In highly oriented pyrolytic graphites (HOPGs), the magnetic ordering was obtained by proton irradiation. Kusakabe *et al* [9] proposed a simplified structure shown in figure 1 to explain the spontaneous magnetism in nanographite ribbon. The carbon atoms are monohydrogenated on the left edge and dihydrogenated on the right edge by proton irradiation. The result of the local spin-density approximation shows that the magnetism originates from the existence of the spin-polarized flatband.

In some carbon systems, electron–electron (e–e) interaction and electron–phonon (e–ph) interaction play important roles in determining their properties [10–15]. For instance, the e–ph interaction can have significant effects on the property of the ground state and can induce

[1] Author to whom any correspondence should be addressed.

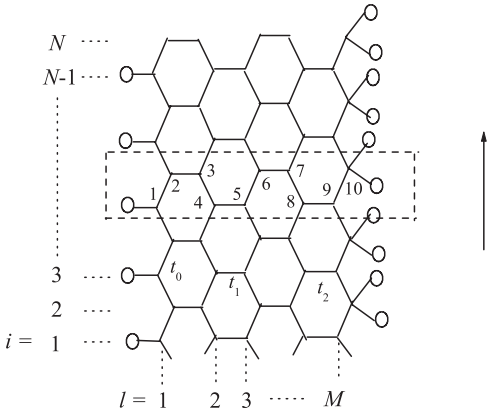

Figure 1. A hydrogenated nanographite ribbon with M zigzag chains each with N carbon atoms. Open circles denote hydrogen atoms and other sites represent carbon atoms. The dashed rectangle denotes a unit cell. The arrow labels the direction of chains.

nonlinear excitations (solitons, polaron). In previous work [16], using the Peierls–Hubbard model, one of the authors has investigated the ferrimagnetism and perfect dimerization in the ground state. A domain wall and the spin soliton in the excited state are also predicted. Because the Coulomb interaction is a long-range interaction, it is important to clarify the effects of long-distance e–e interactions on ferromagnetism in real materials. For carbon nanotubes, a metal–insulator Hubbard transition driven by Coulomb repulsion has been found [11]. Due to the interplay of on-site and intersite Coulomb repulsions U and V, there exist three regions separating a metallic or semimetallic phase and charge-density-wave (CDW) and spin-density-wave (SDW) insulating phases. In nonmagnetic nanographite ribbons with zigzag edges, Yamashiro *et al* [12] found a charge-polarized state with a finite electric dipole moment caused by the interplay between the nearest-neighbour (NN) Coulomb interaction and the edge states. This charge-polarized state competes with the peculiar spin-polarized state caused by the on-site Coulomb interaction.

In this paper, using the Peierls-extended Hubbard model (PEHM) we study the stability and dimerization of the ferromagnetic ground state for the nanographite ribbon in figure 1. We focus on the effects of the NN intersite Coulomb interaction V. It is shown that as V increases to a critical value the ferromagnetic ground state is unstable and the system transits from the SDW state to the CDW state. As the width of the ribbon increases, this critical value changes from the result $U \approx 2V$ from the one-dimensional extended-Hubbard model (EHM) [17, 18] to $U \approx 4V$ from the two-dimensional EHM [19]. As V is enhanced the dimerization first increases to a maximum then reduces to zero. In the one-dimensional EHM, there exists a novel narrow region with bond-order-wave (BOW) phase between the well-known CDW and SDW phase in the ground-state phase diagram [17, 18]. In our PEHM, we also find similar behaviour of the dimerization. For a relative small e–ph coupling, the dimerization which does not exist in the absence of V may appear again in a range of V.

2. Model and computational method

For the nanographite ribbon shown in figure 1, the Peierls-extended Hubbard Hamiltonian is defined as

$$H = H_{\mathrm{t}} + H_U + H_V + H_{\mathrm{el}} \tag{1}$$

$$H_{\rm t} = -\sum_{\langle li,kj\rangle,\sigma} t_{li,kj}(c^{\dagger}_{l,i,\sigma}c_{k,j,\sigma} + {\rm H.c.}) \tag{2}$$

$$H_U = U\sum_{l,i} n_{l,i,\uparrow}n_{l,i,\downarrow} \tag{3}$$

$$H_V = V\sum_{\langle li,kj\rangle} n_{l,i}n_{k,j} \tag{4}$$

$$H_{\rm el} = \frac{\kappa}{2}\sum_{i=1}^{N}\sum_{l=1}^{M-1}(u_{l,i} - u_{l,i+1})^2, \tag{5}$$

where $H_{\rm t}$ is the tight-binding Hamiltonian, H_U is the on-site Hubbard repulsion, H_V is the intersite Coulomb repulsion and $H_{\rm el}$ is the elastic energy due to the lattice distortion along each zigzag chain. Because there is no period in the direction perpendicular to the chain, the interchain distortion does not reduce the total energy of the system as the dimerization in the one-dimensional system does. On the other hand, the two zigzag edges in the nanographite ribbon are not equivalent. Therefore the uncertain interchain deformation does not benefit the energy and is not considered in our model.

In equations (2)–(5), $c^{\dagger}_{l,i,\sigma}$ ($c_{l,i,\sigma}$) and $n_{l,i,\sigma}$ are the creation (annihilation) and number operators of electron with spin $\sigma = \uparrow, \downarrow$ on the ith site in the lth chain, respectively. $n_{l,i} = n_{l,i,\uparrow} + n_{l,i,\downarrow}$. $\langle li, kj\rangle$ labels the nearest neighbours (NNs). $t_{li,kj}$ denotes the hopping integral. U is the on-site e–e interaction, V is the nearest-neighbour e–e interaction. κ is the elastic constant of the lattice. $u_{l,i}$ is the displacement of the ith site in the lth chain. In figure 1, we consider M zigzag chains each with N carbon atoms. The hopping integral in $H_{\rm t}$ is labelled in figure 1. The NN hopping integral along each chain is $t = t_0 - \gamma(u_{l,i} - u_{l,i+1})$, where γ is the electron–phonon coupling constant. t_2 denotes the interchain hopping between the $(M-1)$th chain and the right edge (the Mth chain) while t_1 represents other NN interchain hopping.

Within the Hartree–Fock approximation (HFA), the e–e interaction in the Hamiltonian (1) can be written as

$$n_{l,i,\sigma}n_{k,j,\sigma'} = \langle n_{l,i,\sigma}\rangle n_{k,j,\sigma'} + \langle n_{k,j,\sigma'}\rangle n_{l,i,\sigma} - \langle n_{l,i,\sigma}\rangle\langle n_{k,j,\sigma'}\rangle. \tag{6}$$

Following the procedure in [16], we obtain the self-consistent equations

$$-\sum_{\langle li,kj\rangle} t_{li,kj}Z^{\sigma}_{\mu,k,j} + U\langle n_{l,i,-\sigma}\rangle Z^{\sigma}_{\mu,l,i} + V\langle n_{k,j}\rangle Z^{\sigma}_{\mu,l,i} = \epsilon^{\sigma}_{\mu}Z^{\sigma}_{\mu,l,i} \tag{7}$$

$$\langle n_{l,i,\sigma}\rangle = \sum_{\mu}^{({\rm occ})} Z^{\sigma *}_{\mu,l,i}Z^{\sigma}_{\mu,l,i}, \tag{8}$$

where $Z^{\sigma}_{\mu,l,i}$ is the expansion coefficient of the single-particle wavefunction of the system. ϵ^{σ}_{μ} is the μth eigenvalue of the single-particle state. $\langle n_{l,i,\sigma}\rangle$ is the average with respect to the ground state, and (occ) means those states occupied by electrons.

In following discussion, we define a dimensionless lattice deformation

$$y_{l,i} = \gamma(u_{l,i} - u_{l,i+1})/t_0. \tag{9}$$

$y_{l,i}$ can be obtained by minimizing the total energy

$$y_{l,i} = 2\lambda\left(\sum_{\mu,\sigma}^{({\rm occ})} Z^{\sigma}_{\mu,l,i}Z^{\sigma}_{\mu,l,i+1} - \frac{1}{N}\sum_{i,\mu,\sigma}^{({\rm occ})} Z^{\sigma}_{\mu,l,i}Z^{\sigma}_{\mu,l,i+1}\right), \tag{10}$$

where the periodic boundary condition has been used for each zigzag chain. $\lambda = \gamma^2/t_0\kappa$ is a dimensionless e–ph coupling constant.

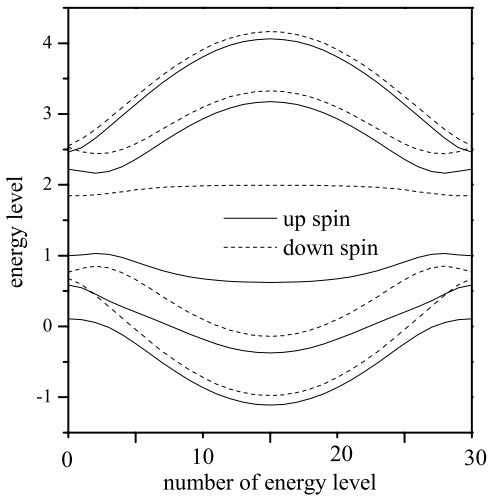

Figure 2. Band structure of the system for $U = 2$, $V = 0.2$, $\lambda = 0.6$, $M = 3$.

3. Results and discussion

For a nanographite ribbon consisting of M zigzag chains each with N carbon atoms, we numerically solve the self-consistent equations (7)–(10). We take the hopping integral $t_0 = 1$ as the unit of energy. In the structure in figure 1, the interchain hopping t_1 is smaller than the intrachain hopping t_0. The π electron at the right edge is relatively localized. As in [16], we take $t_1 = 0.9$ and $t_2 = 0.8$. The band structure of the system with $N = 60$ and $M = 3$ is shown in figure 2 for $U = 2$, $V = 0.2$ and $\lambda = 0.6$. The electron energy spectra contain five down-spin energy bands and five up-spin energy bands since there are five sites in a unit cell. In the ground state, the lowest three up-spin bands and two down-spin bands are filled so that the total spin of the system is $S = \frac{1}{2}$ per unit cell. Due to the energy gap between the highest occupied energy level and the lowest unoccupied energy level, the ferromagnetic ground state is stable.

As the intersite repulsion V increases, the energy gap is reduced. When V is greater than a critical V_c, the gap disappears and the ferromagnetic ground state is unstable. Figure 3 shows the phase diagram in the parameter space of U and V for the e–ph coupling $\lambda = 0.6$ and different width of the ribbon M. Below the curves the ferromagnetic ground state is stable. On increasing the width of the ribbon M, the critical V_c decreases. This means that if V is considered the nearer the system approaches the two-dimensional one the more unstable the ferromagnetic ground state becomes. We will give further discussion on this later.

Figures 4 and 5 show the charge density and spin density for $U = 2$, $M = 5$ and $\lambda = 0.6$. When the intersite Coulomb is turned on, the charge density is redistributed inhomogeneously. With increasing V, the charge density transfers from even sites (sites 2, 4, 6, 8) to odd sites. The charge transfer at the two edges is much larger than that in the middle chains of the ribbon. This result can be understood since the sites at the edges are only subjected to the repulsive interaction of one NN chain while the sites in the middle chains are contemporaneously subjected to the Coulomb repulsion of two NN chains. Another feature in figure 4 is that when V approaches $V_c \approx 0.75$ the charge transfer is strongly enhanced by V. On the other hand, figure 5 indicates that an antiferromagnetic correlation exists between the NN sites. With increasing V, the spin density decreases and the antiferromagnetic correlation

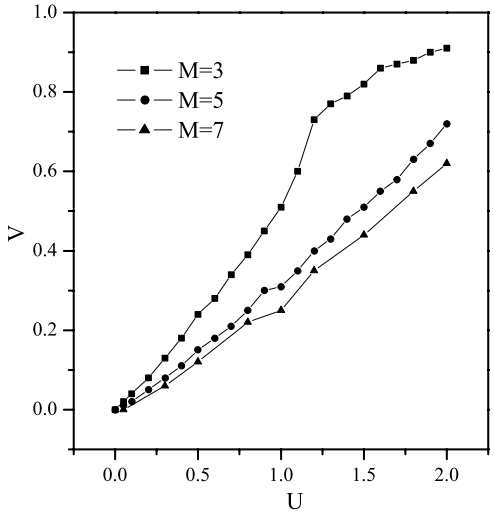

Figure 3. Phase diagram in the parameter space of U and V for $\lambda = 0.6$ and different M.

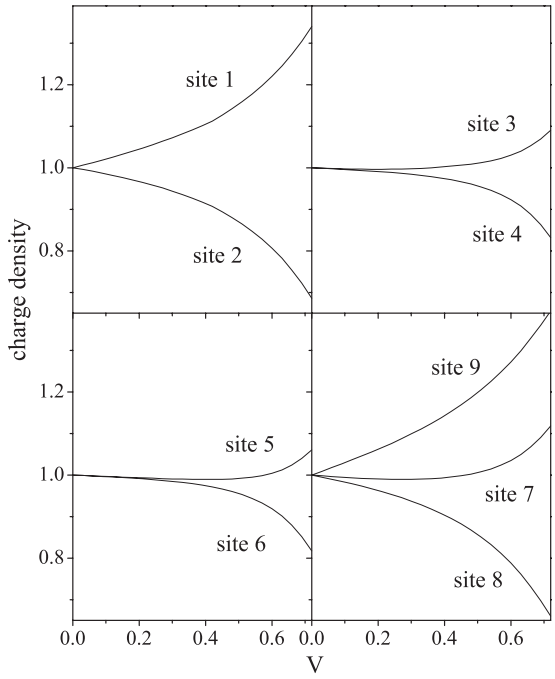

Figure 4. Charge density at different sites in a unit cell versus V for $U = 2$, $\lambda = 0.6$ and $M = 5$.

weakens, especially at the two edges. Combining figures 4 and 5, we conclude that as the intersite Coulomb V increases to its critical value $V_c = 0.75$, the charge distribution exhibits a large polarization while the ferromagnetic state is unstable and the spin polarization is strongly suppressed. This indicates that the system transits from the SDW state to the CDW state.

In the one-dimensional EHM, there exists a transition from the SDW state to the CDW state at $U \approx 2V$ [17, 18]. Figure 3 shows that for a narrow nanographite ribbon (e.g. $M = 3$),

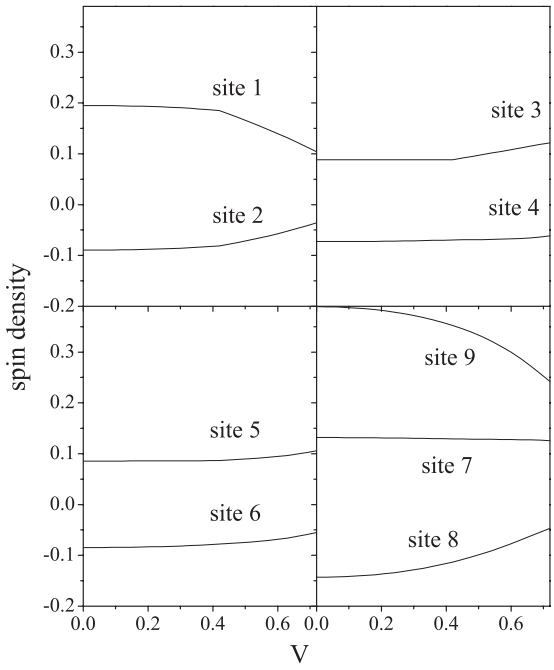

Figure 5. Spin density at different sites in a unit cell versus V for $U = 2$, $\lambda = 0.6$ and $M = 5$.

the transition point is at $U = 2.17V$, which approaches the value for the one-dimensional case. As the ribbon becomes wider, the antiferromagnetic correlation becomes weaker since the total spin per unit cell is still $S = 1/2$ and the spin density at each site decreases. The required intersite Coulomb to overcome this antiferromagnetic correlation decreases. Therefore, the critical V_c in figure 3 is smaller for $M = 5$ and $M = 7$ than that for $M = 3$. In the two-dimensional EHM, the transition from the SDW state to the CDW state is found near $U \approx 4V$ [19]. The result in figure 3 indicates that with increasing the width M of the ribbon, the critical value V_c approaches that in the two-dimensional EHM.

For the Peierls–Hubbard model, due to the interplay between the e–ph coupling λ and the on-site repulsion U, the dimerization may appear in the first zigzag chain [16]. However, if the intersite Coulomb is considered, the behaviour of the dimerization will change. Figure 6 shows the dimerization $y_1 = (-1)^i y_{1,i}$ versus V for different U, λ and M. If the dimerization without V is large (see figure 6(a) for $\lambda = 0.6$), the dimerization hardly changes for small V but reduces rapidly for large V. If the dimerization without V is small (see figure 6(a) for $\lambda = 0.585$), with increasing V the dimerization first increases to a maximum then reduces to zero. In particular, for relatively small λ (see figure 6(a) for $\lambda = 0.58$), the dimerization does not exist for small V. As V increases continuously the dimerization may appear in a range of V. For a narrow ribbon (e.g. $M = 3$) and not too large e–ph coupling, the dimerization always disappears before the transition from the SDW state to the CDW state occurs. Certainly, the dimerization is accompanied by the alternation of bond length. Hence this feature is similar to that in the one-dimensional EHM, in which the BOW phase exists in a narrow range of V between the CDW and SDW states. However, there is obvious difference between these two models. For too small λ, the dimerization does not exist for any V while the BOW phase in the one-dimensional EHM does not require e–ph coupling. The dimerization in the present PEHM

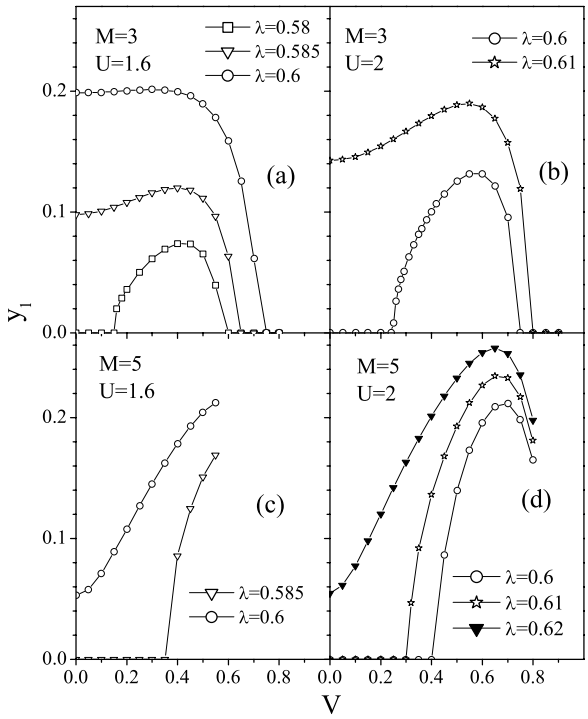

Figure 6. Dimerization y_1 versus V for different U, λ and M.

results from the interplay between λ, U and V while the BOW phase in the EHM exists in a narrow region of U and V.

Comparing figure 6(a) with (b), one finds that for $\lambda = 0.6$, as U increases from 1.6 to 2.0 the dimerization disappears in the absence of V but emerges again in a range of V. This indicates that the on-site repulsion usually suppresses the dimerization, while an appropriate intersite repulsion is in favour of the dimerization. For wider nanographite (e.g. $M = 5$) figures 6(c) and (d) show the dimerization versus V before the energy gap disappears. In these cases, as V is enhanced the transition from SDW to CDW states occurs before the dimerization reduces to zero. The HFA fails to exhibit the results after the disappearance of the gap because of the uncertainty of the occupied states near the Fermi level in each iterative step. Comparing figure 6(b) with (d), it is seen that for given U and λ, the maximum of the dimerization is larger for a wider ribbon than for a narrow ribbon. This behaviour indicates that as the ribbon becomes wider the effect of V is enlarged due to the change in the number of neighbours. A similar enlargement effect with increasing dimension is also found in the transition from SDW to CDW states, which occurs at $V \approx 0.5U$ and $V \approx 0.25U$ in the one- and two-dimensional EHM, respectively.

In summary, for a nanographite ribbon, we have studied the effect of the intersite Coulomb interaction on the stability of the ferromagnetic ground state and the dimerization. As the NN Coulomb interaction increases to a critical value V_c, the ferromagnetic ground state is unstable and a transition from the SDW state to the CDW state occurs. On increasing the width of the ribbon, the critical value V_c changes from $V_c \approx 0.5U$ to $V_c \approx 0.25U$, which are similar values to those in the one- and two-dimensional EHM, respectively. The on-site repulsion usually suppresses the dimerization while an appropriate intersite repulsion is in favour of the

dimerization. In particular, the dimerization may appear in a range of V even if it does not exist in the case of $V = 0$. This indicates that the NN intersite Coulomb can turn the dimerization on off. The behaviour is similar to the effect of the intersite Coulomb on the BOW in the one-dimensional EHM.

Acknowledgments

This work is supported by the National Natural Science Foundation of China under the Grant Nos 50573059 and 10374073, and FANEDD of China under the Grant No. 200034.

References

[1] Iwamura H, Sugawra T, Itoh K and Takui T 1985 *Mol. Cryst. Liq. Cryst.* **125** 379
[2] Takahashi M, Turek P, Nakazawa Y, Tamura M, Nozawa K, Shiomi D, Ishikawa M and Kinoshita M 1991 *Phys. Rev. Lett.* **67** 46
[3] Mukai K, Nedachi K, K, Tamali J B and Achiwa N 1993 *Phys. Lett.* **214** 559
[4] Kawamoto T, Shirai M and Suzuki N 1995 *Synth. Met.* **71** 1789
[5] Tanaka K, Ago H and Yamabe T 1995 *Synth. Met.* **72** 225
[6] Makarova T L, Sundqvist B, Höhne R, Esquinazi P, Kopelevich Y, Scharff P, Davydov V A, Kashevarova L S and Rakhmanina A R 2001 *Nature* **413** 716
[7] Esquinazi P, Spemann D, Höhne R, Setzer A, Han K-H and Butz T 2003 *Phys. Rev. Lett.* **91** 227201
[8] Höhne R and Esquinazi P 2002 *Adv. Mater.* **14** 753
[9] Kusakabe K and Maruyama M 2003 *Phys. Rev.* B **67** 092406
[10] Heeger A J, Kivelson S, Schrieffer J R and Su W P 1988 *Rev. Mod. Phys.* **60** 781
[11] Sancho M P L, Muñoz M C and Chico L 2001 *Phys. Rev.* B **63** 165419
[12] Yamashiro A, Shimoi Y, Harigaya K and Wakabayashi K 2003 *Phys. Rev.* B **68** 193410
[13] Mazumdar S and Dixit S N 1983 *Phys. Rev. Lett.* **51** 292
[14] Campbell D K, Gammel J T and Loh E Y 1990 *Phys. Rev.* B **42** 475
[15] Ma J and Yuan R-K 1997 *Phys. Rev.* B **57** 9343
[16] Wang W Z 2005 *Phys. Rev.* B **71** 094407
[17] Sandvik A W, Balents L and Campbell D 1997 *Phys. Rev. Lett.* **92** 236401
[18] Zhang Y Z 2004 *Phys. Rev. Lett.* **92** 246404
[19] Ohta Y, Tsutsui K, Koshibae W and Maekawa S 1994 *Phys. Rev.* B **50** 13594